Proceedings of IDETC/CIE 2006
ASME 2006 International Design Engineering Technical Conferences &
Computers and Information in Engineering Conference
September 10-13, 2006, Philadelphia, Pennsylvania, USA

DETC2006-99304

ROBUST DESIGN OF COMPRESSOR BLADES AGAINST MANUFACTURING VARIATIONS

Apurva Kumar[*] **A. J. Keane, P. B. Nair**
Computational Engineering and Design Group
School of Engineering Sciences
University of Southampton
Southampton, SO171BJ, UK

S. Shahpar
Aerothermal Methods
Rolls-Royce plc
PO Box 31
Derby, DE248BJ, UK.

ABSTRACT

The aim of this paper is to develop and illustrate an efficient methodology to design blades with robust aerodynamic performance in the presence of manufacturing uncertainties. A novel geometry parametrization technique is developed to represent manufacturing variations due to tolerancing. A Gaussian Stochastic Process Model is trained using DOE techniques in conjunction with a high fidelity CFD solver. Bayesian Monte Carlo Simulation is then employed to obtain the statistics of the performance at each design point. A multiobjective optimizer is used to search the design space for robust designs. The multiobjective formulation allows explicit trade-off between the mean and variance of the performance. A design, selected from the robust design set is compared with a deterministic optimal design. The results demonstrate an effective method to obtain compressor blade designs which have reduced sensitivity to manufacturing variations with significant savings in computational effort.

Keywords: Robust design; multiobjective optimization; surrogate modeling; compressor blades, manufacturing tolerances.

1 INTRODUCTION

Compressor blades are central to the performance of a modern gas turbine engine. They have subtle aerodynamic shapes designed after years of research and insight. However, manufactured blades inevitably show deviation from their intended baseline design shape due to the presence of manufacturing tolerances and errors. This may lead to deteriorated aerodynamic performance and subsequent high in-service cost. Due to limitations of manufacturing processes, decreasing the tolerance limits or reducing machining errors can prove to be very expensive. Hence, it is desirable to design blades that are less sensitive to such effects.

In the presence of prior knowledge about tolerance limits and limitations of the manufacturing processes one can model the manufacturing uncertainty and propagate it through the design system. In recent years, there has been a resurgent interest in computational analysis and design methods that rationally accommodate uncertainty arising from sources such as varying operating conditions and

*ak3@soton.ac.uk

inaccurate system parameters [1]. In most cases, removing the causes of uncertainty can be prohibitively expensive. Robust design methods can be effective as they are concerned with minimizing the effect of uncertainty on design performance without eliminating the source of uncertainty [2].

In the 1970s Taguchi emphasized the need to reduce variation in products and processes to improve their quality [3,4]. An overview of Taguchi's experimentation strategy and parameter design method can be found in [5,6]. The system design method and the selection of Signal-to-Noise Ratio (SNR) as a measure of robustness proposed by Taguchi had several limitations [7,8]. Welch et al [9,10] proposed a system for quality improvement via computer experiments as an alternative to Taguchi's method. Statistical decision theory has also been used to formulate robust design as an optimization problem. The minimax strategy [11] can be used to find a design with optimal worst case performance [12]. This method is conservative as it seeks to protect the decision maker against the worst case scenario [8]. Huyse et al [13, 14] used the idea of Bayes risk minimization to achieve consistent improvement of the performance over a given range of uncertainty parameters.

Many researchers have proposed minimizing a single objective to achieve robust design. These methods can be classified into two categories where the aim is to minimize (1) the expectation of the objective function in its neighborhood [14–17], and (2) the variance of the objective function [18, 19]. Tsutsui et al [15] used a genetic algorithm based method with perturbations in the phenotype while evaluating the function value. They call this method Genetic Algorithms with Robust Solution Searching Schemes (GAs/RS^3), which they further combine with a sharing scheme to seek multiple robust solutions. Jin et al [20] provide a survey of evolutionary optimization based methods for seeking robust optimal designs. Garzon et al [21] present two formulations for robust design of a compressor cascade. In the first formulation they minimize the expectation of the performance while in the second they minimize the variance of the performance with a constraint on the expectation.

The robust design approach proposed here combines an efficient multiobjective optimization algorithm with a parametric geometry model, Computational Fluid Dynamics (CFD) and surrogate models. The motivation behind this hybrid strategy is to ensure convergence close to the true Pareto front using a limited number of function evaluations. In the approach presented here, Design of Experiment (DOE) techniques are used to create an initial dataset. A parametric geometry model and grid generator are combined to generate meshes which are then used for CFD simulations. NSGA-II [22] is then used in conjunction with a Gaussian stochastic process model to search the design space for Pareto-optimal solutions. The mean and standard deviation at each design search point in evaluated using Bayesian Monte Carlo Technique (BMCS). A sequential search strategy is used to update the surrogate model as the optimization proceeds. The proposed method is applied to seek compressor fan blade sections that have robust performance in the presence of manufacturing uncertainty. Detailed numerical studies are presented for robust geometric design of a typical compressor fan blade.

2 MODELING AND PARAMETRIZATION

To model manufacturing uncertainty we need to find a method which can describe geometry variations in a given tolerance band around the nominal geometry. These could be variations in chord, camber and thickness. Most of the existing airfoil parametrization techniques are limited to modeling variation in camber and thickness. Here we present an efficient method using combination of Hick-Hennes functions and splines for modeling manufacturing variations. To parametrize the blade section geometry we use a linear combination of Hicks-Henne functions super-imposed on a baseline shape. For the problem under consideration, we have used 10 Hicks-Henne functions, five each for the upper and lower airfoil section, to parametrize the compressor fan blade. The Hicks-Henne shape functions can be expressed as

$$b_i(x) = sin^4(\pi x^{m_i}) \; , \;\; m_i = ln(0.5)/ln(x_{M_i}) \quad \text{where } i = 1, 2, ...n \tag{1}$$

where x is the normalized chord-wise coordinate starting from the trailing edge encompassing the whole airfoil and back to the trailing edge. $(0 \leq x \leq 1)$, x_{M_i} are preselected-selected values corresponding to the location of the maxima and n is the number of Hicks-Henne functions used. In the present study, the locations of x_{M_i} for $i = 1, 2, ..., 5$ are chosen in a manner to ensure clustering near the leading edge. This ensures more points where the curvature is higher and thus more variety in shapes near the leading edge. Furthermore, two control points required are chosen to be the two points at the cusp on the trailing edge. This ensures that we also achieve deviations in the chord length of the airfoil.

These shape functions are added to a typical Rolls-Royce compressor fan blade section to obtain new shapes. They are added along the normals which are evaluated by fitting local cubic polynomials at the locations of interest. The amplitudes of these shape functions are used as design variables and hence, for our design study we have 10 design variables. The design space is judiciously selected such that the minimum thickness constraints along the chord are satisfied in an implicit manner. Figure 1 shows typical variations in geometry caused by changing design variables.

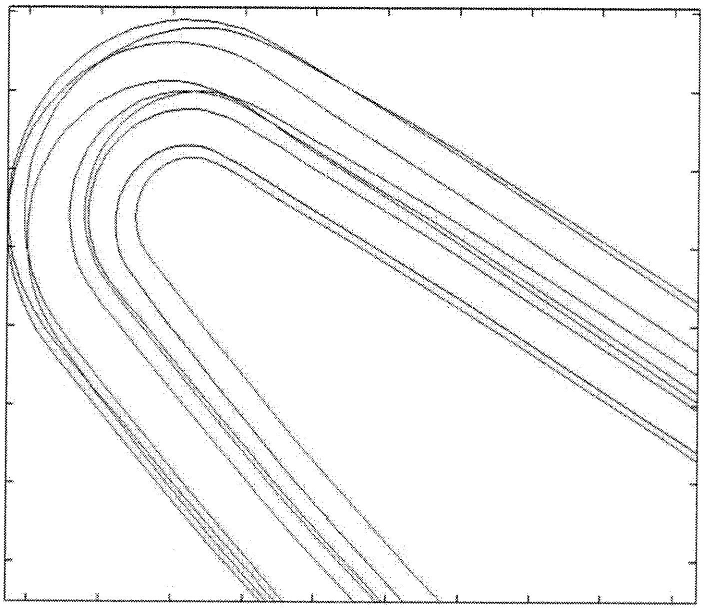

Figure 1. Typical compressor blade shapes generated using the proposed parametrization technique

Robust design methods require the definition of noise factors and control factors in the system design. In this case the 10 design variables can be used as the control factors and small perturbations in these design variables can be treated as noise variables. This idea can be very useful when used in conjunction with surrogate models. As the noise factors space is a subset of the control factor space, a single DOE run can be employed to train the the global surrogate which can then be employed for further design analysis. Figure 2 shows a tolerance band around the nominal geometry that is representative of typical tolerances observed in manufacturing compressor blades.

3 AERODYNAMIC ANALYSIS

Once the parametrized geometry model is developed it is combined with the Rolls-Royce propriety code PADRAM, a parametric design and meshing routine employed for automating the geometry creation and grid generation process [23]. PADRAM makes use of both transfinite interpolation and elliptic grid generation to generate hybrid C-O-H meshes. An orthogonal body fitted O mesh is used to capture the viscous region of the airfoil whilst an H mesh is used near the boundary where stretched cells are required, for example in the wake region. After grid refinement studies we select a mesh of the order of 28,000 cells in two dimensions. Figure 3 shows a typical CFD grid used for the present study.

A non-linear, unstructured viscous flow solver HYDRA is used for the CFD simulation [24]. It solves the Reynolds Averaged steady Navier-Stokes (RANS) equations with the Spalart-Allmaras turbulence model. To accelerate convergence to steady-state HYDRA employs a multigrid algorithm with preconditioning [25]. A four level multigrid is used for the present simulations. The inlet boundary conditions for the CFD analysis are Total temperature = 290 Kelvin, Total Pressure = 63400 Pascal, Whirl Angle = -37.28 Degrees and the outlet boundary condition is Static Pressure = 52000 Pascal. An initial uniform flow condition with Density = 0.7675 kg/m^3, Velocity = 0 and Pressure = 66932 Pascal is considered. The converged CFD solution is used to calculate the pressure loss at the nominal geometry and typically takes 1200 seconds (0.5 hour) using a Intel(R) Xeon(TM) CPU 3.06GHz dual processor machine. The equation

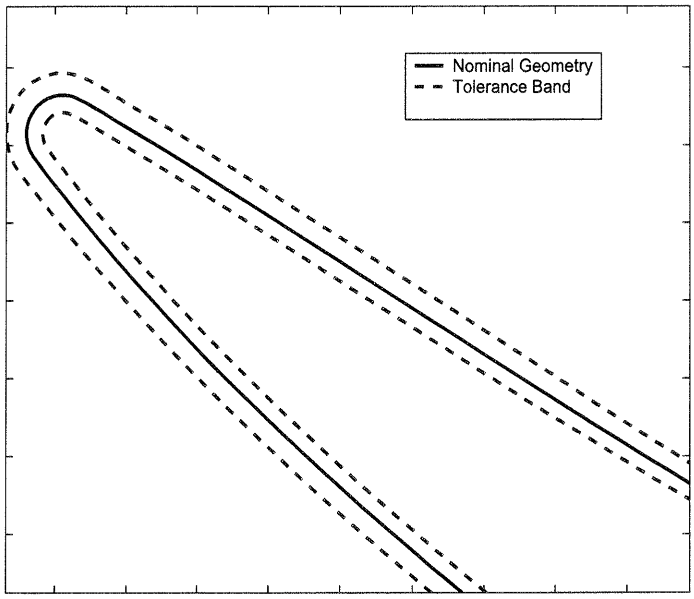

Figure 2. Small perturbations in the design variables within the tolerance band is used to model the manufacturing variations at each design point

for the pressure loss is:

$$Loss = \frac{P_{inlet} - P_{exit}}{P_{inlet}} \times 100 \tag{2}$$

where P_{inlet} is the total pressure at the inlet and P_{exit} is the total pressure at the exit. Figure 4 shows the pressure contour plot for a selected compressor blade geometry.

4 PROBABILISTIC PERFORMANCE ANALYSIS

This sections starts with an overview of the Gaussian Stochastic Process Model which is used in this study as a computationally cheap surrogate to the high fidelity CFD simulation. The methodology for training the surrogate model using DOE and high fidelity CFD runs, and its application for analyzing the aerodynamic performance is presented. Finally, the surrogate model is employed for probabilistic analysis of a typical Rolls-Royce compressor blade in the presence of manufacturing variations using Bayesian Monte Carlo (BMCS) technique [26]. The need for Robust Optimization in the design phase is emphasized. The savings in computational effort for this analysis as compared to the direct use of CFD code is also discussed.

4.1 Surrogate Modeling

The computational cost associated with high-fidelity simulation rules out the direct application of the MCS technique for probabilistic analysis. Surrogate modeling uses the basic idea of analyzing an initial set of design points to generate data which can be used to construct computationally cheap approximations of the original high-fidelity model. The CFD simulator used for high-fidelity analysis in this study can be represented by the functional relationship $y = f(\mathbf{x})$, where $\mathbf{x}$ is the vector of inputs to the simulation code and y is the output. The objective is to construct an approximate model $\widehat{y} = \widehat{f}(\mathbf{x}, \alpha) \approx f(\mathbf{x})$, that is computationally cheaper to evaluate. α is a vector of undetermined hyperparameters which is estimated using the input-output dataset $\{\mathbf{x}^{(i)}, y^{(i)}\}, i = 1, 2, \ldots, n$. In general, surrogate modeling involves the following steps: (1) data generation, (2) model structure selection, (3) parameter estimation and (4) model validation. A detailed exposition of these steps can be found in [26].

In the present study we use a Gaussian stochastic process model as a surrogate to the high-fidelity CFD simulation code. This

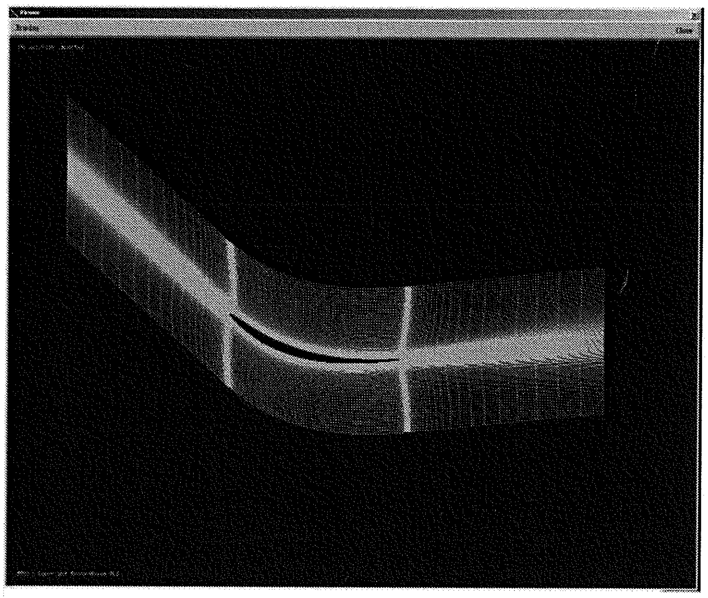

Figure 3. A Typical C-O-H Mesh used for CFD analysis

approach was originally developed in the field of geostatistics (where this approach is referred to as Kriging) and has been in use since the early 1960s [27]. It is also widely used in the neural network community where it is referred to as Gaussian process regression [28,29]. The model structure typically used in Gaussian stochastic process modeling can be expressed as

$$Y(\mathbf{x}) = g(\mathbf{x}) + Z(\mathbf{x}). \tag{3}$$

The above model is a combination of a global model ($g(\mathbf{x})$) and a local model ($Z(\mathbf{x})$). $g(\mathbf{x})$ is usually a linear or quadratic polynomial function, however, a constant $g(\mathbf{x}) = \beta$ is often found to be sufficient for modeling complex functions. $Z(\mathbf{x})$ is a Gaussian random function with zero mean and non-zero covariance and is used to model the local deviations from the global model, i.e.,

$$\mathsf{Mean}(Z(\mathbf{x})) = 0 \text{ and } \mathsf{Cov}(Z(\mathbf{x}), Z(\mathbf{x}')) = \Gamma(\mathbf{x}, \mathbf{x}') = \sigma_z^2 R(\mathbf{x}, \mathbf{x}'). \tag{4}$$

In other words, the observed outputs of the simulation code $\mathbf{y} = \{y^{(1)}, y^{(2)}, ..., y^{(n)}\}$ are assumed to be realizations of a Gaussian random field with mean β and covariance Γ. Here $R(.,.)$ is a parametrized correlation function that can be tuned to the training dataset and σ_z^2 is the so called process variance.

A commonly used choice of covariance function is the stationary family which obeys the product correlation rule [30].

$$R(\mathbf{x}^{(1)}, \mathbf{x}^{(2)}) = \prod_{j=1}^{p} \exp(-\theta_j |\mathbf{x}_j^{(1)} - \mathbf{x}_j^{(2)}|^{\gamma_j}), \tag{5}$$

where $\theta_j \geq 0$ and $1 < \gamma_j \leq 2$ are the hyperparameters. In theory, the choice of an optimal covariance function is data dependent. However, in practice it has been found that the parametrized covariance function in Eq. (5) offers sufficient flexibility for modeling smooth as well as nonlinear functions [31]. If a Gaussian process prior over functions is used, the posterior process is also Gaussian. Hence using

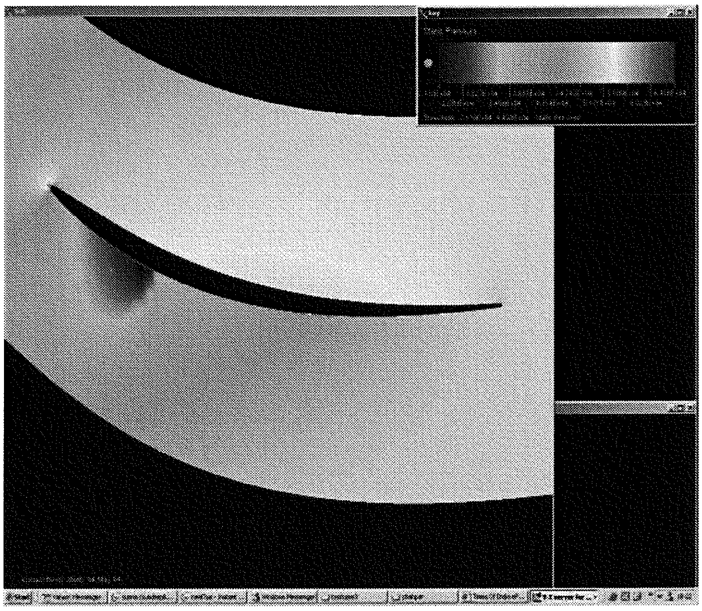

Figure 4. CFD Pressure Contour Plot

standard results from Bayesian inferencing, the posterior mean and covariance can be stated as

$$\hat{y}(\mathbf{x}) = \beta + \tau(\mathbf{x})^T \mathbf{R}^{-1}(\mathbf{y} - \mathbf{1}\beta), \tag{6}$$

and

$$C(\mathbf{x}, \mathbf{x}') = \sigma_z^2 \left(R(\mathbf{x}, \mathbf{x}') - \tau(\mathbf{x})^T \mathbf{R}^{-1} \tau(\mathbf{x}') \right). \tag{7}$$

Here $\mathbf{R}$ is the correlation matrix whose ijth element is calculated as $R(\mathbf{x}^{(i)}, \mathbf{x}^{(j)})$, $\tau(\mathbf{x}) = \{R(\mathbf{x}, \mathbf{x}^{(1)}), R(\mathbf{x}, \mathbf{x}^{(2)}), ..., R(\mathbf{x}, \mathbf{x}^{(n)})\}^T \in \mathbb{R}^n$ and $\mathbf{1} = \{1, 1, ..., 1\}^T \in \mathbb{R}^n$. The hyperparameters $\theta, \beta, {\sigma_z}^2$ are computed from the training dataset via maximum likelihood estimation, which involves solving the following optimization problem

$$\{\theta, \beta, {\sigma_z}^2\} = \arg \max_{\{\theta, \beta, {\sigma_z}^2\}} \frac{1}{2} \left[n \ln(2\pi) + n \ln \sigma_z^2 + \ln |\mathbf{R}| + \frac{1}{\sigma_z^2} (\mathbf{y} - \mathbf{1}\beta)^T \mathbf{R}^{-1} (\mathbf{y} - \mathbf{1}\beta) \right]. \tag{8}$$

In the numerical studies presented here, we use a hybrid GA to solve the above optimization problem.

It may be noted from Eqs. (6) and (7) that the Gaussian stochastic process modeling approach finally leads to an approximation of the high-fidelity computational model as a multidimensional Gaussian random field. The posterior variance $\sigma^2(\mathbf{x}) = C(\mathbf{x}, \mathbf{x})$, can be interpreted as an estimate of the uncertainty involved in predicting the output at any new points using the given finite dataset. One key advantage of this approach is that the user can get an estimate of the prediction error, which can be exploited in optimization procedures to sequentially update the surrogate model and hence improve its predictive capability [26, 32].

4.2 Numerical Analysis

To construct a Gaussian process surrogate model, we carry out a 150 point LP_τ [26] DOE survey over the values design variables. The parameters of the perturbed geometry are specified by upper and lower bounds. The automated grid generator and CFD simulator are run to evaluate the pressure loss at each design point. The scatter plot of the values of pressure loss are shown in Fig. 5.

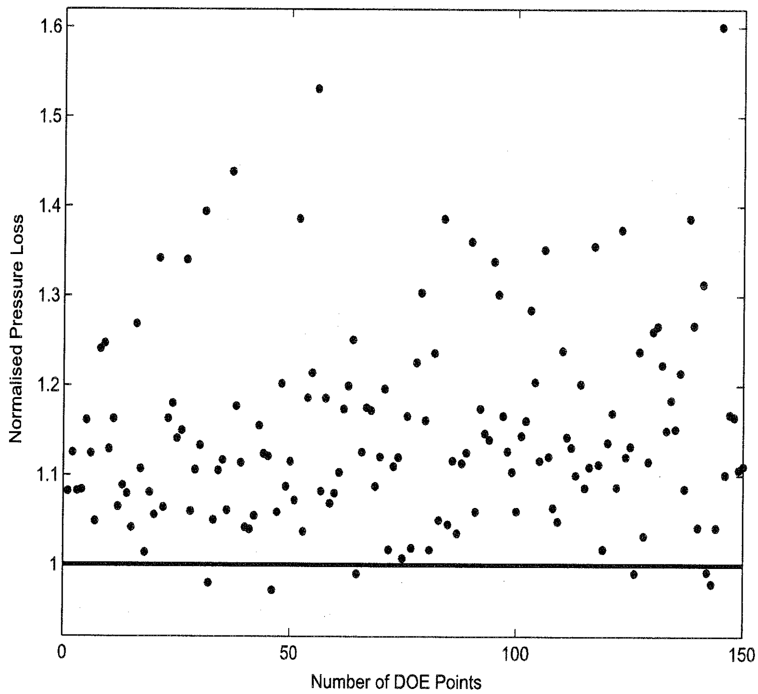

Figure 5. The Scatter Plot of Pressure Loss using the training dataset

The surrogate is employed to study the effect of manufacturing variations on the baseline geometry. Bayesian Monte Carlo Simulation (BMCS) [26] is employed to simulate the manufacturing process for the baseline geometry. A normal distribution for the noise variables is assumed with the tolerance limits assigned to lie at $[-3\sigma, +3\sigma]$. A 10,000 point BMCS is run using the surrogate model to generate the probability distribution of the pressure loss. The histogram for the pressure loss is shown in Fig. 6. The BMCS using the surrogate model takes less than 10 seconds to carry out 10,000 evaluations on an Intel(R) Xeon(TM) CPU 3.06GHz dual processor machine. This shows substantial savings in computational time, as compared to using the high-fidelity CFD model for probabilistic studies which would have taken 12000000 seconds (3333.34 hours) for the same analysis. This study suggests that manufacturing variations can deteriorate the aerodynamic performance of a blade significantly. In the worst case there can be 20% degradation in pressure loss coefficient. It also suggests almost 9% shift in mean performance from the nominal performance. These figures re-emphasize the need for robust design strategies for compressor blades in the presence of manufacturing variations.

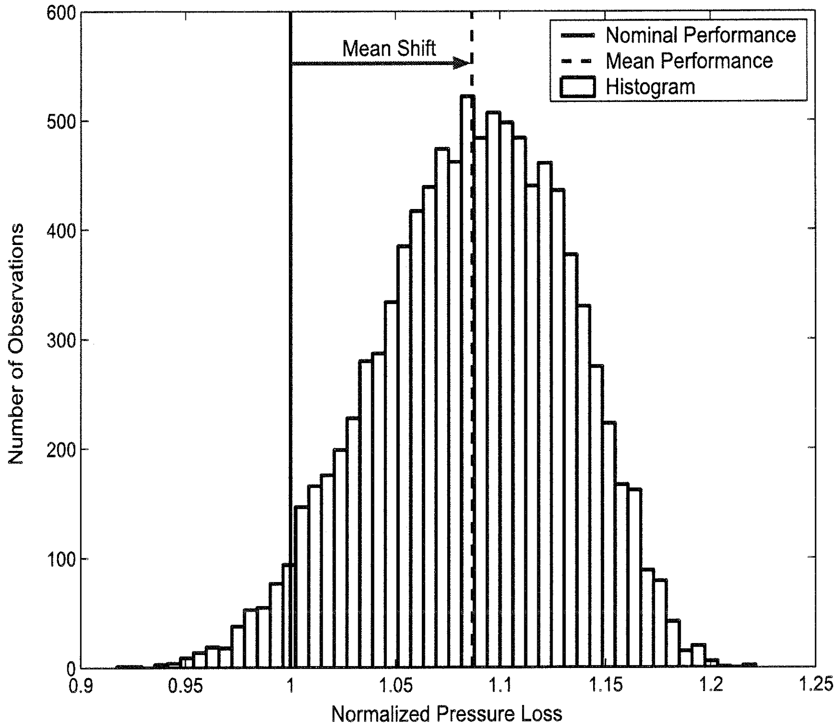

Figure 6. Histogram of aerodynamic performance in the presence of manufacturing uncertainty

5 ROBUST DESIGN METHODOLOGY

Robust design can be formulated as a multi-objective problem with the goal of simultaneously minimizing the mean and standard deviation of the performance, i.e.,

$$\begin{aligned} &\text{Minimize} : \mu = \tfrac{1}{k}\textstyle\sum_{i=1}^{k} Pl_i \quad \text{and} \\ &\text{Minimize} : \sigma = \sqrt{\tfrac{1}{k-1}\textstyle\sum_{i=1}^{k}(Pl_i-\mu)^2}, \quad i = 1,2,\ldots k. \end{aligned} \tag{9}$$

where Pl is the pressure loss and k is the number of perturbed compressor blade types used for representing the noise (manufacturing variations) space. The presence of multiple objectives in a problem leads to a set of Pareto optimal solutions, rather than a single solution. Each point in the set is optimal in the sense that no improvement can be achieved in one objective without worsening the other objective. In the absence of further information about the relative importance of the objectives, it is not possible to decide which design is better than the rest. Hence, it is important to find as many Pareto-optimal solutions as possible for the benefit of the designer.

Classical optimization methods suggest converting the multiple objective optimization problem to a single objective optimization problem emphasizing one particular Pareto-optimal solution at a time. Such methods prove to be computationally expensive and do not ensure convergence to true optimal Pareto sets in non-convex problems [33,34]. In contrast, GAs are inherently suited for multi-objective problems as they have the ability to find multiple Pareto-optimal solutions in one simulation run. Since GAs work with a population of solutions, it is easier to extend them to maintain high diversity in finding multiple Pareto-optimal solutions at each stage, while moving toward the true Pareto-optimal region [35].

In recent years several approaches have been proposed to solve multi-objective problems using GAs [36–39]. The elitism based NSGA-II proposed by Deb et al [22] is employed here to seek the Pareto-optimal front. The NSGA-II method is fast since it has a computational complexity of $O(MN^2)$ (where M is the number of objectives and N is the population size) when compared to other

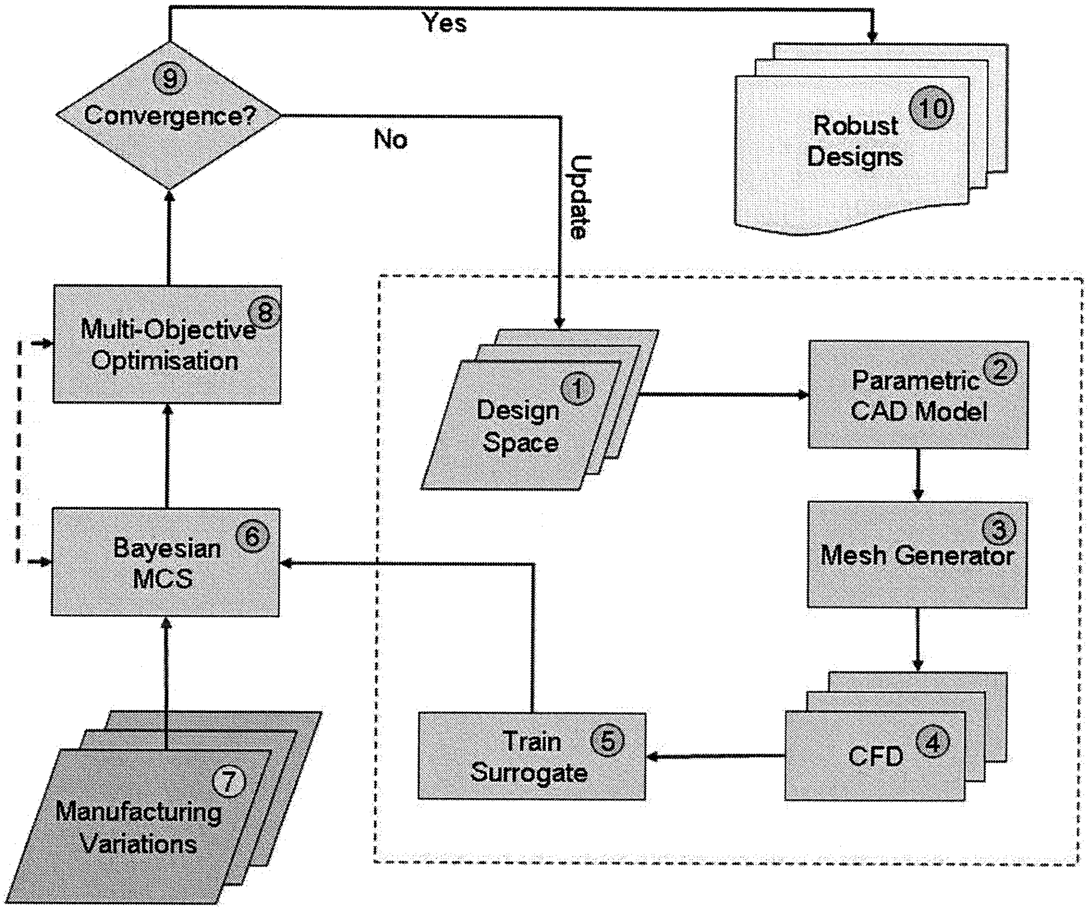

Figure 7. Flowchart for Robust Design method against manufacturing uncertainty

non-dominated GAs with computational complexity $O(MN^3)$. The NSGA-II method also uses elitism to enhance the performance of the GA and prevent the loss of good solutions once they are found. Traditional GA methods ensure diversity in a population by relying on the concept of sharing. In such methods it is necessary to specify the sharing parameter (σ_{share}) beforehand by the user. The performance of sharing functions in ensuring diversity is dependent upon the choice of σ_{share}. In practice it is not very obvious how to select the best value of σ_{share}. In NSGA-II the sharing function approach is replaced by a crowded comparison approach. The crowded comparison approach has a lower computational complexity and eliminates any user defined parameter for maintaining diversity among population members. In this study NSGA-II is employed in conjunction with surrogate models to identify the Pareto-optimal front to seek robust designs.

In the robust design method employed we first select the design space and use DOE techniques to rationally choose a set of compressor fan blade sections as m initial candidate points. These blades are modeled using the parameterization method discussed earlier in this paper. PADRAM is used to produce high quality hybrid meshes and the multigrid RANS solver HYDRA with Spalart Allmaras turbulence model is used for CFD simulations to calculate the total pressure loss over the compressor blade sections. The resulting dataset is used to train a Gaussian Stochastic Process Model which is used as a computationally less expensive surrogate to the high fidelity CFD code. The hyperparameters $\theta, \beta, \sigma_z^2$ of the surrogate model are estimated via maximum likelihood estimation. The mean and standard deviation of the total pressure loss at each design point (over the noise variables) is evaluated using a 10,000 point BMCS.

Unlike conventional robust design procedures we do not limit ourselves to just searching the initial design space. NSGA-II is used in conjunction with the surrogate model to search the entire design space to obtain Pareto-optimal solutions, see Fig. 7. The prediction, using the surrogate model, at the points on the Pareto-front are then verified by running full scale CFD simulations. The errors in the prediction can be estimated from the posterior variance given by the surrogate model at each point. A low-crowding algorithm, which maximizes the euclidean distance between the Pareto points, is used to select points for update. In this study, the process is terminated after three updates. Figure 8 shows the initial dataset, subsequent updates points and the final Pareto Front after three updates. Significant improvement in Pareto front as compared to the initial Pareto front is obtained.

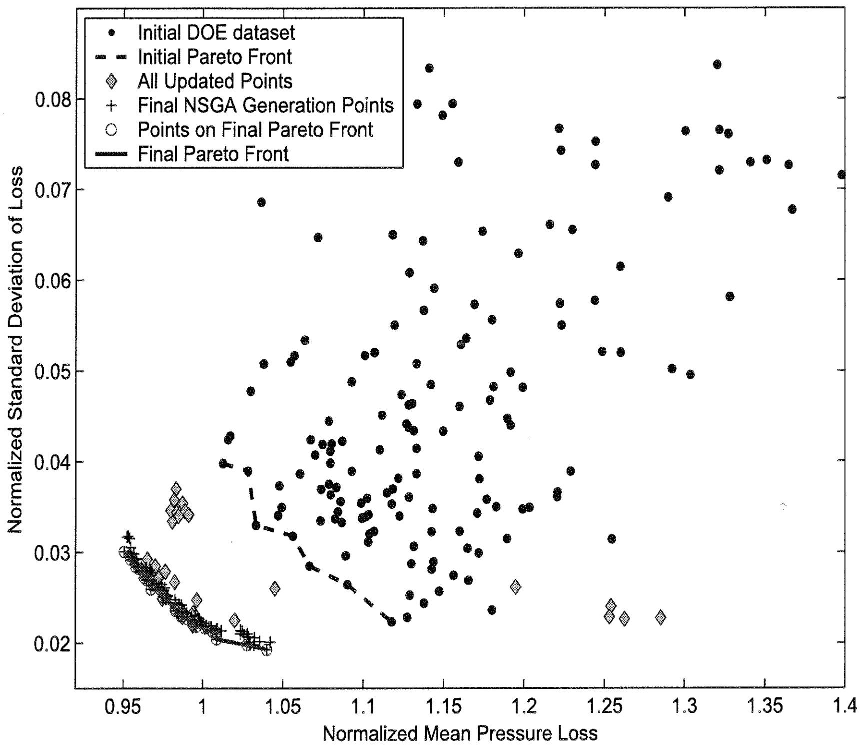

Figure 8. Plot showing initial initial dataset, initial Pareto front, updated points, final NSGA generation points and final Pareto Front. Each point in the plot is evaluated by simulating a manufacturing process with tolerances using BMCS.

6 COMPARISON WITH DETERMINISTIC DESIGN

It is sensible to compare the Robust Blades obtained with a deterministically optimized blade to understand the trade-offs obtained. To provide a benchmark against which the results of a multiobjective robust design search can be compared, we perform a traditional deterministic optimization study. Deterministic design methods seek to optimize the nominal performance of the system, i.e., optimize blade geometries for low pressure loss coefficients. A simulated annealing algorithm, with direct search employed for initial guess, is employed. This search is performed in conjunction with the surrogate model and the initial dataset. A Robust Design from the final Pareto Set is selected for comparison. The selected point is shown in Fig. 9.

The total pressure loss for the deterministically optimal blade and Robust Blade is verified using CFD solution. The nominal performance of the deterministically optimal blade is better as compared to the Robust Blade. BMCS of 10,000 points over the manufacturing variations (noise space) is performed for both the designs. Figure 10 shows the comparison in the performance of the two blades. As expected, the optimal blade obtained from the deterministic optimization has better nominal performance but the performance deteriorates

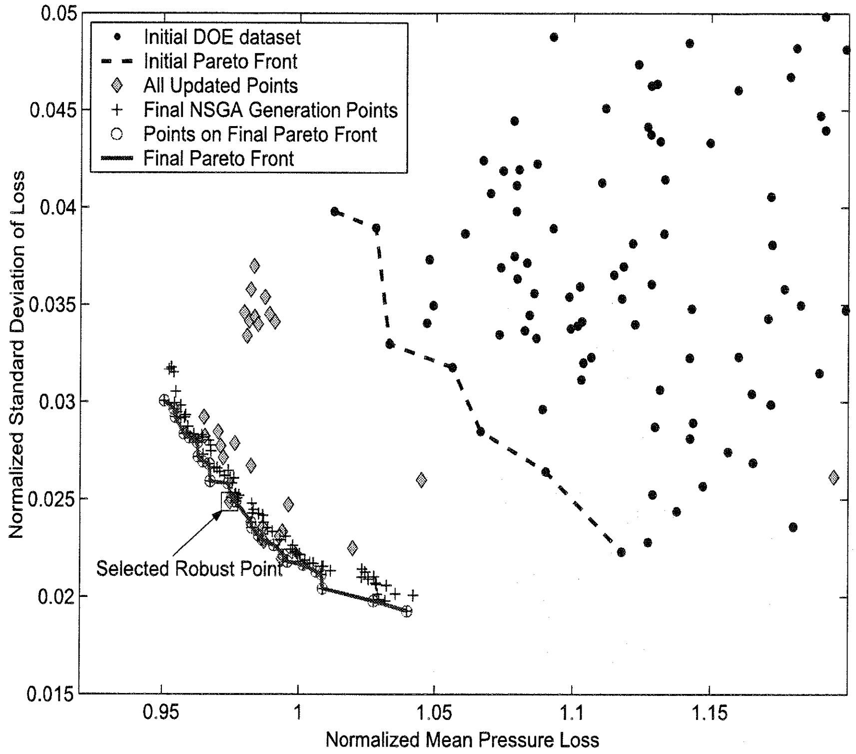

Figure 9. Zoomed in view of the Final Pareto Front. The Robust Design selected for comparison in highlighted with a black box

Blade Designs	Nominal Performance	Mean Performance	Standard Deviation	Mean Shift	Worst Case Performance
Baseline	1.0	1.0865	0.0455	8.65%	1.2109
Deterministic	0.9253	0.9806	0.0430	5.53%	1.1749
Robust	0.9497	0.9748	0.0272	2.51%	1.1662

Table 1. Comparison between the Baseline, Deterministically Optimal and Robust Design

significantly in the presence of manufacturing variations. The histogram of the robust geometry shows less variability in pressure loss coefficient as compared to the design obtained using a deterministic approach.

There is also a considerably lower shift in the mean performance of 2.51% from the nominal performance for the robust blade geometry as compared to almost 5.5% for the deterministic optimal blade geometry, see Table 1. The standard deviation of the Robust blade [$\sigma = 0.0272$] is almost half the standard deviation of the deterministically optimal blade [$\sigma = 0.0430$]. It can be observed that low variability has been achieved in the robust design at the expense of a marginal reduction in the nominal performance. However, the mean performance of the robust blade [$\mu = 0.9748$] is better than the mean performance for the deterministically Optimal blade [$\mu = 0.9806$]. The worst case performance of the robust blade geometry is also almost 1% better than the deterministic optimal blade geometry. Figure 11 shows the zoomed in view of the baseline, deterministic optimal and robust design. The robust design is thus better in all respects except the nominal performance which has very low probability of realization in practice (approximately 3% from figure 10).

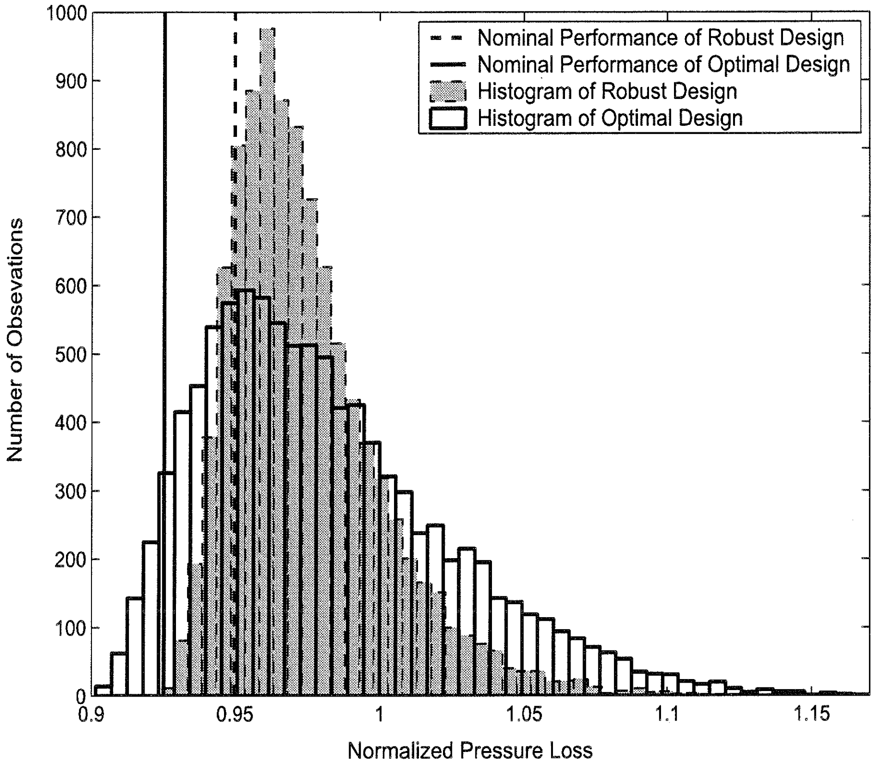

Figure 10. Comparison using histograms of performance of Optimal and Robust Blade

7 CONCLUSION

An efficient genetic algorithm based robust design methodology for compressor blades against manufacturing variations is presented. A novel parametrization method was developed to simulate blade manufacturing process with variations within tolerance bands. LP_τ based DOE technique was used to construct an initial training dataset. A parametric grid generation routine was used to automate geometry creation and grid generation to construct high quality CFD meshes which were then solved using a RANS code. Gaussian stochastic process models were used as computational surrogates to the high-fidelity CFD simulations for conducting BMCS. This ensured improvements in the Pareto front using a limited number of exact function evaluations.

A Robust Design from the final Pareto set was selected for comparison with a deterministically optimal blade design. A BMCS based on the surrogate model was executed for the selected blades and the robust design was found to be considerably less sensitive to manufacturing variations as compared to the deterministic optimal design. The robust design was also found to have better performance than deterministic optimal design in all respects, [Mean, Standard Deviation, Mean Shift, Worst Case Performance], except the nominal performance. Significant computational savings for the robust design studies by employing efficient surrogate models instead of high fidelity CFD simulations was also reported.

ACKNOWLEDGMENT

This work was supported by the University Technology Partnership for Design, a collaboration between Rolls-Royce Plc., BAE Systems and the Universities of Sheffield, Cambridge and Southampton.

REFERENCES

[1] Zang, T., Hemsch, M., Hilburger, M., Kenny, S. P., Luckring, J., Maghami, P., Padula, S., and Stroud, W., 2002. Needs and Opportunities for Uncertainty-Based Multidisciplinary Design Methods for Aerospace Vehicles. Technical Report NASA/TM-

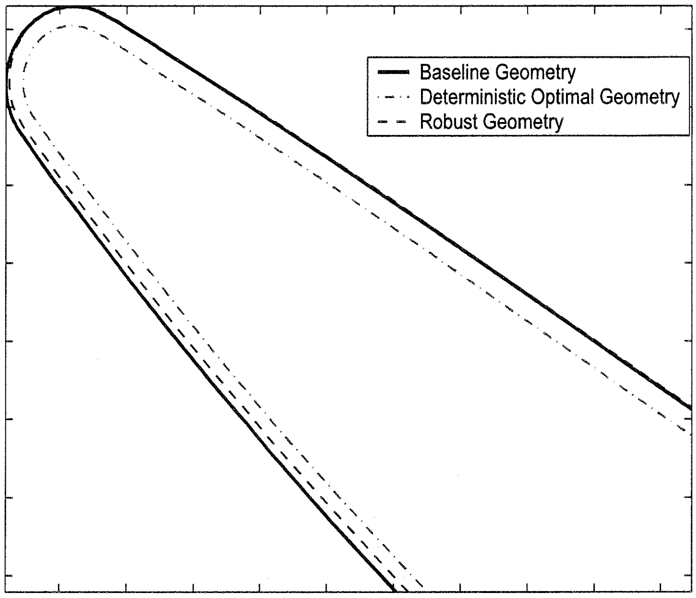

Figure 11. Zoomed in view of the Baseline, Deterministic Optimal and Robust Design Blades

2002-211462, NASA Langley Research Center, Hampton, VA, July.

[2] Phadke, M. S., 1989. *Quality Engineering using Robust Design.* Prentice Hall, New Jersey.

[3] Taguchi, G., and Wu, Y., 1980. *Introduction to Off-Line Quality Control.* Central Japan Quality Control Association, Nagoya, Japan.

[4] Taguchi, G., 1986. *Introduction to Quality Engineering.* UNIPUB/Krauss International, New York.

[5] Nair, V. N., 1992. "Taguchi's parameter design: A panel discussion". *Technometrics,* **34**, pp. 127–161.

[6] Trosset, M. W., 1996. Taguchi and Robust Design. Technical Report 96-31, Houston, Texas.

[7] Box, G., 1988. "Signal-to-noise ratios, performance criteria, and trnaformations (with discussions)". *Technometrics,* **30**(1), p. 1:17.

[8] Trosset, M., Alexandrov, N., and Watson, L., 2003. "New methods for robust design using computer simulations". *American Statistical Association.* Proceedings of the Section on Physical and Engineering Science.

[9] Welch, W., Yu, T., Kang, S., and Sacks, J., 1990. "Computer experiments for quality control". *Journal of Quality Technology,* **22**, pp. 15–22.

[10] Welch, W., and Sacks, J., 1991. "A system for quality improvement via computer experiments". *Communications in Statistics-Theory and Methods,* **20**, pp. 477–495.

[11] Ben-Tal, and Nemirovski, A., 1997. "Robust truss topology design via semidefinite programming". *SIAM Journal of Optimization,* **7**, pp. 991–1016.

[12] Gunawan, S., and Azarm, S., 2004. "Non-gradient based parameter sensitivity estimation of single objective robust design optimization". *ASME Journal of Mechanical Design,* **126**, pp. 395–402.

[13] Huyse, L., and Lewis, R., 2001. Aerodynamic shape optimization of two-dimensional airfoils under uncertain operating conditions. Technical Report NASA/CR-2001-210648, NASA Langley Research Center, Hampton, VA, January.

[14] Li, W., Huyse, L., and Padula, S., 2002. "Robust airfoil optimization to achieve drag reduction over a range of mach numbers". *Structural and Multidisciplinary Optimization,* **24**, pp. 38–50.

[15] Tsutsui, S., and Ghosh, A., 1997. "Genetic algorithms with a robust solution searching scheme". *IEEE Transactions on Evolutionary Computation,* **1**, pp. 201–208.

[16] Tsutsui, S., Ghosh, A., and Fujimoto, Y., 1996. "A robust solution searching scheme in genetic search". In Proceedings of Parallel Problem Solving in Nature, pp. 543–552.

[17] Huyse, L., 2001. "Solving problems of optimization under uncertainty as statistical decision problem". *AIAA 2001-1519.*

[18] Parkinson, D., 1997. "Robust design by variability optimization". *Quality and Reliability Engineering International,* **13**, pp. 97–

102.
[19] Al-Widyan, K., and Angeles, J., 2005. "A model-based formulation of robust design". *ASME Journal of Mechanical Design,* **127**, pp. 388–396.
[20] Jin, Y., and Branke, J., 2005. "Evolutionary optimization in uncertain enviornments: A survey". *IEEE Transactions on Evolutionary Computation,* **9**(3), pp. 303–317.
[21] Garzon, V. E., 2003. "Probabilistic Aerothermal Design of Compressor Airfoils". PhD Thesis, Massachusetts Institute of Technology.
[22] Deb, K., Pratap, A., Agarwal, S., and Meyarivan, T., 2002. "A fast and elitist multiobjective genetic algorithm: NSGA-II". *IEEE Transactions of Evolutionary Computation,* **6**, pp. 182–197.
[23] Shahpar, S., and Lapworth, L., 2003. "Parametric design and rapid meshing systems for turbomachinery optimisation". *ASME-GT2003-38698.*
[24] Moinier, P., 1999. "Algorithm developments for an Unstructured Viscous Flow Solver". PhD Thesis, Oxford University, Oxford.
[25] Moinier, P., Muller, J. D., and Giles, M. B., 1999. "Edge-based multigrid and preconditioning for hybrid grids". *AIAA-99-3339.*
[26] Keane, A., and Nair, P., 2005. *Computational Approaches for Aerospace Design.* John Wiley and Sons.
[27] Matheron, G., 1963. "Principles of geostatistics". *Economic Geology,* **58**, pp. 1246–1266.
[28] Neal, R. M., 1996. *Bayesian Learning for Neural Networks.* Springer.
[29] MacKay, D. J. C., 1997. Guassian processes - a replacement for supervised neural networks. Tutorial lecture Notes for NIPS, at http://www.inference.phy.cam.ac.uk/mackay/abstracts/gp.html.
[30] Jones, D. R., Schonlau, M., and Welch, W. J., 1998. "Efficient global optimization of expensive black-box functions". *Journal of Global Optimization,* **13**(4), pp. 455–492.
[31] Nair, P. B., Choudhary, A., and Keane, A. J., 2001. "A bayesian framework for uncertainty analysis using deterministic black-box simulation code". *AIAA-2001-1676.*
[32] Keane, A., 2003. "Wing optimization using design of experiment, response surface, and data fusion methods". *Journal of Aircraft,* **40**, pp. 741–750.
[33] Athan, T., and Papalambros, P., 1996. "A note on weighted criteria methods for compromise solutions in multi-objective optimization". *Engineering Optimization,* **27**(2), pp. 155–176.
[34] Koski, J., 1985. "Defectiveness of weighting method in multicriterion optimization of structures". *Communications is Applied Numerical Methods,* **1**, pp. 333–337.
[35] Fonseca, C., and Fleming, P., 1993. "Genetic algorithm for multi-objective optimization: Formulation, discussion and generalization.". Proceedings of the Fifth International Conference on Genetic Algorithms. S. Forrest, Ed.
[36] Horn, J., Nafploitis, N., and Goldberg, D., 1994. "A niched pareto genetic algorithm for multi-objective optimization". Proceedings of the First IEEE Conference on Evolutionary Computation. Z. Michalewicz, Ed.
[37] Deb, K., 1999. "Multi-objective genetic algorithms: Problem difficulties and construction of test functions". *Evolutionary Computation,* **7**, pp. 205–230.
[38] Zitler, E., and Thiele, L., 1999. "Multiobjective evolutionary algorithms: A comparitive case study and the strength pareto approach". *IEEE Transactions on Evolutionary Computation,* **3**, pp. 257–271.
[39] Fieldsend, J., Everson, R., and Singh, S., 2003. "Using unconstrained elite archives for multiobjective optimization". *IEEE Transactions on Evolutionary Computation,* **7**, pp. 305–323.

